Auxilia Ruby Sagaya Irudayaraj, Felicita Florence John, Divya Priya Chinnasamy, Kanmani Raman, Amala Infant Joice Joseph*

PG and Research Department of Chemistry, Holy Cross College (Autonomous), Affiliated to Bharathidasan University, Trichy-620002, Tamilnadu, India

Scientific paper
ISSN 0351-9465, E-ISSN 2466-2585
https://doi.org/10.62638/ZasMat1188

Zastita Materijala 66 (1)
90 - 101 (2025)

Synthesis and characterization of *Selenicereus undatus* extract mediated nano-Bi_2O_3 and its application in the adsorption of Rhodamine B dye

ABSTRACT

Betacyanins(BC) arereddish-purple pigment widely found in the peels of white-fleshed dragon fruit (Selenicereus undatus) and peels and pulps ofred-fleshed dragon fruit (Selenicereuscostaricensis). BC pigments are good anti-oxidants that inhibit the formation of reactive oxygen species (ROS) in plants and thereby promote the reduction of metal ions to zero valent metals. It also acts as a good stabilising and capping agent in the synthesis of nanoparticles. Hence, this research aims to extract, and quantize the content of BC from the peels of Selenicereusundatus, to fabricate betacyanin rich-Selenicereusundatus (SU) modified bismuth oxide nanoparticles (Bi_2O_3 NPs) and characterize using UV-Vis, FTIR, XRD, SEM, EDAX and BET. The quantity and stability of the betacyanin are optimized using various parameters like time, temperature, solvent ratio, pH, etc., through UV-Vis spectrophotometer at 538 nm. SynthesizedSU-Bi_2O_3 NPs aims for the alleviation of synthetic dye contaminantsthrough adsorption- an efficient route for water remediation. The nano-adsorbent Bi_2O_3 NPs showed increase in dye adsorption with an increase in reaction time, temperature and Bi_2O_3 NPs dosage, enabling efficient removal of dyes such as Rhodamine B (RhB) dyes.

Keywords: *Betacyanin, selenicereus undatus, bismuth oxide nanoparticles, characterization, Rhodamine B dyes.*

1. INTRODUCTION

The green extract obtained from plant parts, microbes and biomass are used as a non-toxic, eco-friendly reducing and stabilizing agent for the synthesis of metal nanoparticles (M NPs) or metal oxide nanoparticles (M_XO_Y NPs). The bioactive compound present in the green extract reduces the metal ions to the required M NPs or M_XO_Y NPs. One such bioactive compound that attracts the recent research field is the 'Bioactive Natural Colorant'. The food and textile industries seek interest in natural colorants (NC) to promote non-toxic replacement and at the same instant health beneficial products. Major parts of NC are obtained from plant sources like bark (oak dye), roots (madder dye), leaves (indigo), flowers (saffron, hibiscus, butterfly pea and marigold lavender) fruits (dragon fruit, beets, berries and red cabbage) and also from microbes (Streptomyces coelicolor, Actinorhodin)[1,2]. The common bioactive pigments responsible for the color of the dyes are anthocyanin, betalain, carotenoids and chlorophyll.

Among them, betalains are found to show antioxidant, detoxicant and readily get adsorbed and digested in humans. Betalains is a water-soluble nitrogen-containing NC with two types-yellow pigment (betaxanthins) and reddish-violet pigment (betacyanins) found exclusively in the order Caryophyllales which includes, beets, amaranth, pitayas, cactus pear, swiss chard, etc. Besides, replacing synthetic dyes into NC requires overcoming some limitations like high expense, poor stability and poor staining in clothes. The peel of pitayas, both red fleshed(Selenicereus costaricensis) and white fleshed (Selenicereus undatus) contains high content BC which is usually discarded as waste. From the peels of pitayas, BC(Figure 1) can be extracted using water as a solvent and estimate the quantity through spectroscopic techniques [3]. However, these pigments are unstable by their nature and need optimization of a few parameters like temperature, time, solvent nature, dilution and pH.

*Corresponding author: Auxilia Ruby Sagaya Irudayaraj
E-mail: auxiliaruby@gmail.com
Paper received: 05.06. 2024.
Paper accepted: 01.07. 2024.

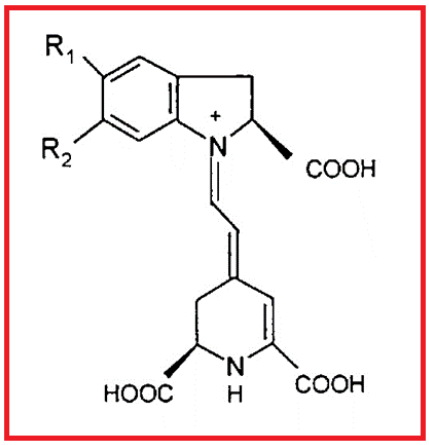

Figure 1. Structure of betacyanins

In the synthesis of nanoparticle, certain features like stability, shape, size and surface area depends on the reduction potential of ions which was governed by the nature of plant extract. Green synthesized MNPs showed vast applications in the field of biomedical, catalysis, adsorption, biosensors, nano-sensors, drug delivery, fertilizer delivery, gene delivery, harmless cosmetics, crop protection and water remediation[4]. Bismuth oxide nanoparticles (Bi_2O_3) (Figure 2) showed considerable advances in many fields of application due to peculiar properties like high surface area, wide band gap, elevated refractive index, high levels of electrical properties and good diamagnetism. Existing polymorphs of Bi_2O_3 are α-Bi_2O_3(monoclinic), β-Bi_2O_3(tetragonal), γ-Bi_2O_3(bcc), δ-Bi_2O_3(fcc cubic), ε-Bi_2O_3(metastable related to α- and β-phase), ω-Bi_2O_3(triclinic). The most stable form at room temperature is monoclinic- α phase $Bi_2O_3$and others are high-temperature phases. Due to the high surface area of Bi_2O_3, it acts as a good nano-adsorbent in the removal of various pollutants like dye, pesticides, fertilizers, heavy metals, industrial effluents, soaps and detergents[5].

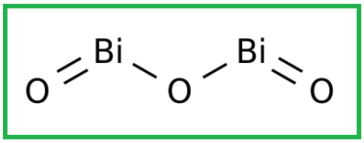

Figure 2. Structure of bismuth oxide

The discharge of dyes into the biosphere, mutilates mankind through dermatitis, carcinogenic, asthmatic disorder, nausea and colon polyps. Stability and resisting power of dyes makes it difficult to degrade by oxidants, photocatalyst, microbes and electrochemical destruction. Adsorption via nanotechnology is a coherent, eminent and advantageous method [6].Hazardous effluents like dyes, heavy metals, Volatile organic compounds (VOCs), pathogens, polymers, radio-active sediments etc., are engulfed all over the water bodies.Synthetic dyes ruin the grandeur features of water via inhibiting photosynthesis, disrupt the biological cycle and promoting skin toxi-city, Septicemia, bone deformities, carcinogenicity and neurological problems. One such menacing dye is Rhodamine B (RhB) which wascategorized as group 3 carcinogenic by International Agency for Research on Cancer (IARC) and also banned its use as artificial food colorant in India[7]. Thus water remediationthrough nano-sorbent is an efficient strategy to demolish ubiquitously available contaminants especially dye abolition.

2. EXPERIMENTAL SECTION:

2.1. Separation of peels from the pulp of Selenicereusundatus (SU):

White dragon fruit *(Selenicereusundatus) was* purchased from the farms of Dharmapuri district, Tamil Nadu, India. The fruit was washed with tap water to remove all the dust and microbes. Further rinsed with DD water for 2 to 3 times and separated the peel part from flesh using a clean knife. The non-red parts like flower end pit, bracts, areole are removed completely. Even though the pulp of the fruit was removed, yet it still contained some white fibers like structure, which was also removed. Finally, the peels were chopped into cubes (1-2 cm) and stored at low temperature for extraction.

2.2. Extraction of BC from the peels of SU:

Quantification of BC was achieved by treatingthe peels with DD water as extraction solvent. Dependence of extraction condition was scrutinized by assorting solvent-peel ratio (5:1, 7.5:1, 10:1, 12.5:1, 15:1, 17.5:1, 20:1, 22.5:1 and 25:1), temperature of extraction (30°C, 40°C, 50°C, 60°C, 70°C, 80°C, 90°C, 100°C, 110°C and 120°C), duration of extraction (0.5 hr, 1 hr, 1.5 hrs, 2 hrs, 2.5 hrs, 3 hrs, 3.5 hrs, 4 hrs, 4.5 hrs, 5 hrs) and pH ranges (1, 2, 3, 4, 5, 6, 7, 8, 9, 10, 11, 12). The above acquired extracts were filtered using Whatman no.1 filter papers and refrigerated until further processing.

2.3. Determination of BC from SU peels extract:

Absorbance of individual peel extract was determined using Visican Spectrophotometer-type 167 at wavelength 538 nm which corresponded to BC pigment [8].

Quantification of BC (mg/100 g) =

$A_{(at\ 538\ nm)}$. м. D. υ. 100/ε. ш. ⌊

where,

$A_{(at\ 538\ nm)}$=Absorbance at 538 nm corresponding to BC

ʍ= Molecular weight of BC ≈ 550g mol^{-1}

D=Dilution factor

ʊ= Volume of extract (in ml)

ε=Molar absorption coefficient $6x10^6$ L mol^{-1} cm^{-1}

ɯ=Gram weight of *SU*peels taken.

ǀ=Path length ≈ 1 cm

2.4. Green synthesis of Bi_2O_3NPs:

Green synthesis of Bi_2O_3NPs was carried out using the optimized*Selenicereusundatus*peels extract. About 10ml of *Selenicereusundatus*extract was added to 0.1M $Bi(NO_3)_3$and stirred continuously for 2hrs at 90℃. Initially, the color of the solution appeared champagne pink and the pH measured 6. Once the pH was increased to 10, the solution start to precipitate and color turnedto pale yellow. After completion of the reaction, the precipitate was centrifuged 3-4 times with ethanol and DD water, dried in hot air oven for 2 hrs and calcinated in muffle furnace for 3hrs at 300℃.

2.5. Characterization of green Bi_2O_3NPs:

Green synthesized Bi_2O_3NPs were characterized by P-XRD (PANalytical X'Pert Pro) to analyze the structural modification with Cu-Kα radiation source ranged from 0°to 90°. XRD helps in determining the crystal structure, nature of crystallinity, lattice parameters, orientation etc., based on the diffraction patterns obtained. Particle size could be identified from the peaks, as the size decreases, the peak gets broadened. Further it was analyzed using FTIR spectrophotometer (Perkin Elmer Spectrum Two) with $LiTaO_3$ detectors. Anhydrous KBr optical transparent salt was used to make pellets with Bi_2O_3 NPs of 13 mm diameter using hydraulic press machine (kimaya-table top). FTIR measured the absorption/ Transmittance of the IR radiation produced by the sample at range 4000cm^{-1} to 400cm^{-1}. Furthermore, UV-Visible spectrophotometer for Bi_2O_3NPswas recorded using Perkin Elmer Lambda 35 with range 190nm-1100nm. Nanoparticles have unique optical characters that affect the size, shape, agglomeration, refractive index etc., which makes UV-Visible spectrophotometer, an efficient tool for characterizing. Additionally, the morphology of the green synthesized Bi_2O_3NPswas studied using SEM (Carel Zeiss-EVO 18). Enhanced topology information was provided by BSD detectors on EVO 18. High resolution of SEM helps to focus and magnify closely packed specimen and provides a visual ideology of shape and size. EDAX helped to identify the elements present in the material and its composition. This technique reassured the presence of required elements with less or no impurities. BET surface area analysis was carried out for Bi_2O_3 NPs using BETSORP Max-Microtrac BEL. Adsorption capacity of Bi_2O_3NPs was tested using N_2 as adsorbate. Known amount of N_2 was passed over the sample till saturation pressure attains and the adsorption layer formed was detached byheating to estimate the desorption process. The obtained data wasexhibited as BET isotherm[9].

2.6. Adsorption studies of Bi_2O_3NPs

Adsorption properties of green Bi_2O_3NPs were investigated using Rhobamine B dye with various concentrations, time of contact, temperature and pH. Based on these factors, the adsorption capacities were measured and the best adsorption behaviours of the nanoparticles were identified minimizing the factors affecting adsorption. Various adsorption processes were carried out at disparate physical conditions are tabulated belowin table 1.

Table 1. List of various adsorption parameters and ranges utilized for adsorption studies

Adsorbent dosage (NPs)	20mg	50mg	100mg	150mg	200mg	250mg
Adsorbate dosage (RhB dye)	10ppm	20ppm	30ppm	40ppm	50ppm	60ppm
Adsorption time	30mins	45mins	1hr	1.5 hrs	2hrs	2.5hrs
Adsorption Temperature	30℃	40℃	50℃	60℃	70℃	80℃
Adsorption pH	1	3	5	7	9	11

3. RESULTS AND DISCUSSION

3.1. Optimization of BC quantity

3.1.1. Optimization of BC based on solvent-peel ratio

The solvent-peel ratio was varied (5:1, 7.5:1, 10:1, 12.5:1, 15:1, 17.5:1, 20:1, 22.5:1, 25:1) and for each extraction process, approximately 1gof peels was added to the required DD water at 40°C for 2 hrs.Based on the absorbance obtained at λ=538 nm for the above solutions, its BC quantity was determined using the equation (1).

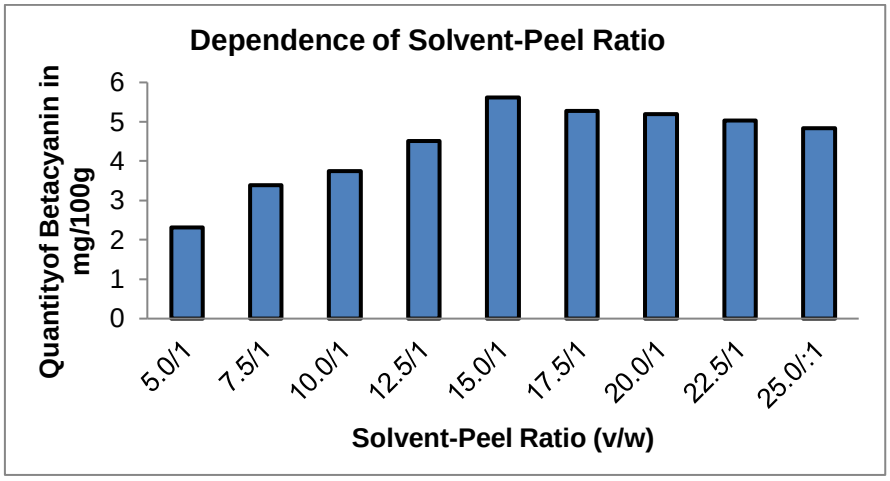

Figure 3. Plot depicting the correlation between Solvent-Peel ratio and BC quantity

Figure 3 represents the quantity of BC modification with respect to the solvent-peel ratio. BC quantity was highest for 15:1 with 5.63 ±0.15 mg of BC content per 100 g of fresh peels of *Selenicereusundatus.*BC being a water-soluble pigment it required an enough quantity of solvent to dissolve it. Hence solvent-peel ratio below 15:1 shows low BC quantity due to insufficient solvent. If the solvent is increased over the optimum condition, no change or slight decrease in BC content, proving that the most suitable solvent-peel ratio is 15:1.

3.1.2. Optimization of BC based on Temperature

BC pigments were highly unstable to thermal condition because it undergoes degradation resulting in decreases in the quantity of BC. Extraction process was carried out with solvent-peel ratio 15:1 and temperature varied from 30°C to 120°C for 2 hrs. Figure 4 represents the quantity of BC with respect to the temperature variation. Optimum temperature for this case was found to be 50°C with BC content 5.87± 0.22 (mg/100g) and further increase leads to a gradual decrease in the quantity of BC. Temperature from 30°C to 50°C showed an increase of BC content because it facilitates diffusion of pigment into solvent. Additional increase of temperature beyond the optimum condition might lead to degradation of pigments resulted in decrease of BC content upto 1.99± 0.11 (mg/100g).

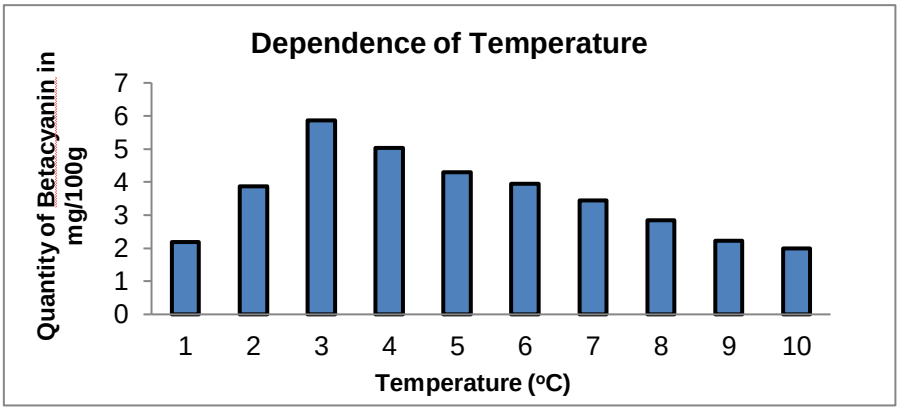

Figure 4. Plot depicting the correlation between Temperature and BC quantity

3.1.3. Optimization of BC based on Time

The dependence of time was illustrated in figure 5. In order to analyse the influence of extraction time, solvent-peel ratio of 15:1 was utilized at temperature 50°C for various time periods (30mins, 1hr, 1hr 30mins, 2hrs, 2hrs 30mins, 3hrs, 3hrs 30mins, 4hrs, 4hrs 30mins and 5hrs). The optimum condition with maximum extraction of BC was found at 3hrs with quantity 4.31± 0.13 (mg/100g). When extraction time increases, naturally the BC content increases and reaches a maximum (at pH-6). Beyond this point, hydrolyzes occurs leading to the formation of betanidine, betalamic acid, aminesand ultimately decreases BC content.

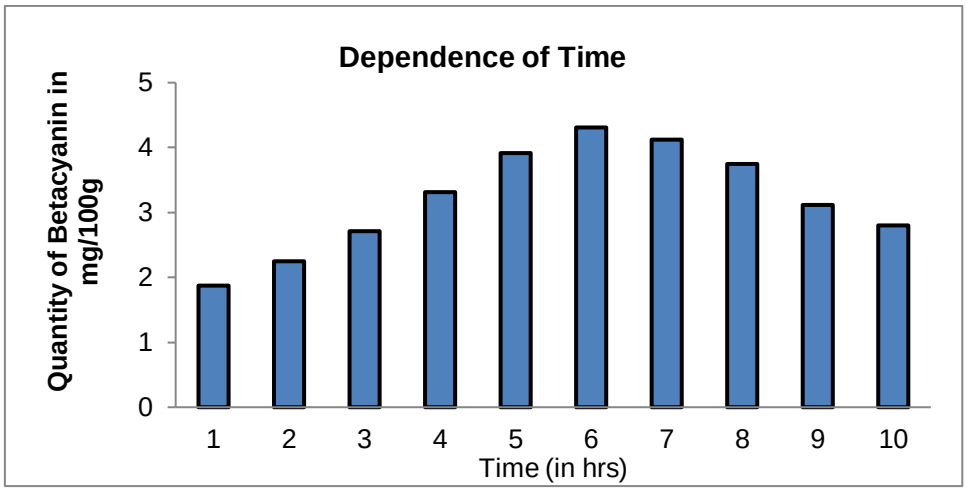

Figure 5. Plot depicting the correlation between Time and BC quantity

3.1.4. Optimization of BC based on pH

To analyse the dependence of pH, extraction processes was carried out with solvent-peel ratio 15:1, at temperature 50°C for 3hrs with pH range from 1.0 to 12.0. Figure 6 represents the correlation between pH and BC quantity. BC pigments show optimal stability at pH 5.0-6.0. This study coincides with the previous theories, and showed maximum BC quantity at pH 6.0 with 3.02 ± 0.19 (mg/100g). Both acidic and basic condition for BC is non-favorable. In acidic medium, the color change to yellow because of re-condensation of betalamic acid with amino acid residues. In basic medium decomposition of betanidin occurs [10].

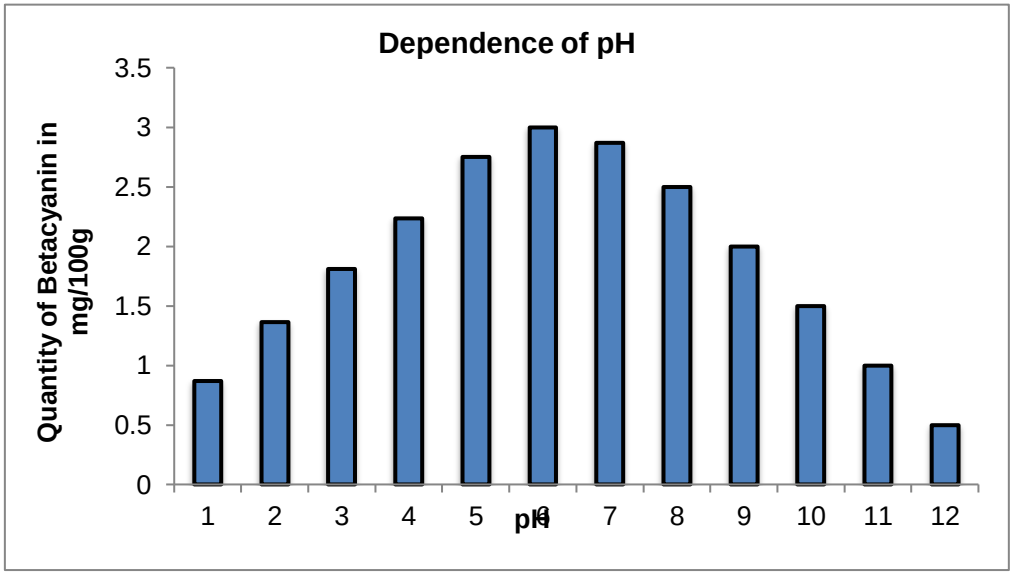

Figure 6. Plot depicting the correlation between pH and BC quantity

3.2. Characterization of Bi_2O_3NPs

3.2.1. UV-Visible Spectroscopy

The UV-Vis spectrum of the green synthesized Bi_2O_3 NPs was given in Figure 7. The sharp absorption peak observed at 290nm confirmed the formation of Bi_2O_3NPs [11] and the band gap of Bi_2O_3 NPs was 3.31 eV calculated using the formula, $Eg = 1240/\lambda_m$, where λ_m represented the maximum absorbance value.

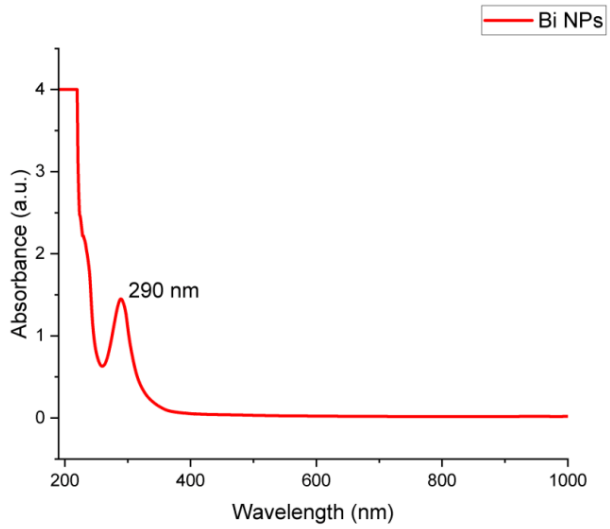

Figure 7. UV-Visible spectrum of Bi_2O_3NPs

3.2.2. FT-IRSpectroscopy

The FTIR spectrum was recorded in the range of 400 – 4000 cm^{-1} to determine chemical bonding and qualitative formation of green synthesized Bi_2O_3 NPs, portrayed in figure 8. The O–Hstretching vibrations appeared at 3436.11 cm^{-1}. The active ingredient in *Selenicereus undatus* is betacyanin pigment (figure1) and the peaks at 2926 cm^{-1}, 1634.47cm^{-1} and 1389.88 cm^{-1} represents C-H stretching, N-H bend (1º amine) and C-C stretching (aromatics) respectively. The characteristic vibrational modes for metal-oxygen bonding are usually found below 1000 cm^{-1}[12]. Bi_2O_3 NPs has two bonding vibration (Bi-O and Bi-O-Bi) and their peaks are found at 845.69 cm^{-1}, 509.99 cm^{-1} and 433.65 cm^{-1}.

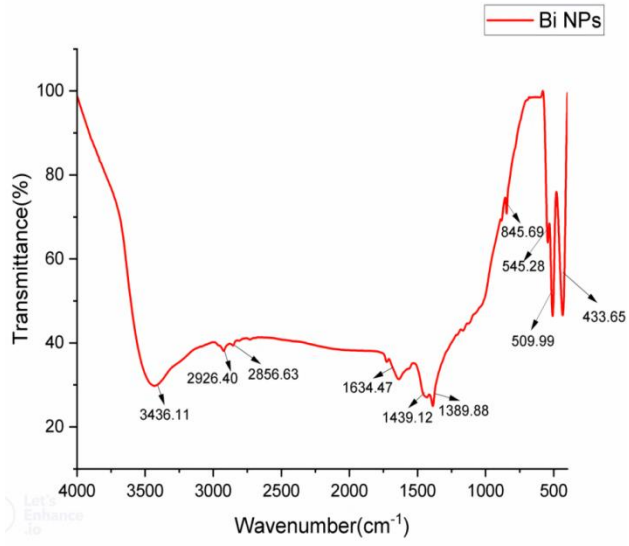

Figure 8. FTIR of Bi_2O_3NPs

3.2.3. X-Ray Diffraction of Bi_2O_3NPs

The crystalline nature and structural composition were illustrated through powder XRD studies of Bi_2O_3NPs measured from diffraction angle 5° to 90°. XRD spectrum of Bi_2O_3 NPs has been shown in figure 9 which showed sharp diffraction angles (2Θ) at 6.55°, 12.33°, 19.65°, 23.31°, 26.28°, 27.87°, 29.45°, 33.01°,37.10°, 39.33°and 42.79° which corresponded to the miller indices of the reflecting angles (110), 020), (102), (111), (120), (012), (212), (121), (112), (131) and (122) respectively [13]. All the peaks could be indexed to the standard Joint Committee on Powder Diffraction Standards (JCPDS) card no.76–1730 and no additional peaks were obtained, proclaims the purity and absence of unstable polymorphs. The XRD pattern manifest the monoclinic structure of Bi_2O_3 which was the most stable allotropes and it was denoted as α-Bi_2O_3. The sharp peaks manifested the high crystalline nature and the crystalline size was ~122.16 nm, calculated using Debye-Scherrer equation, where (120) plane being the maximum intense plane was utilized as Θ value [14].

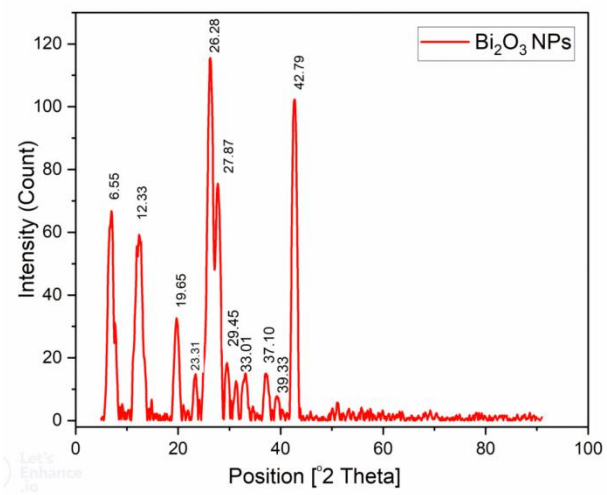

Figure 9. XRD pattern of Bi_2O_3NPs

3.2.4. Scanning Electron Microscope image of Bi_2O_3NPs

The morphology and size of bismuth oxide nanoparticles were analyzed using SEM. Figure 10 represented the SEM image of Bi_2O_3NPs with resolution on the order of 1µm -100nm and magnification range from 10KX to 50KX magnification which showed that the particles are poly-dispersed structures having smooth surface area. The particle size calculated from the SEM micrograph ranged from 120-130 nm.

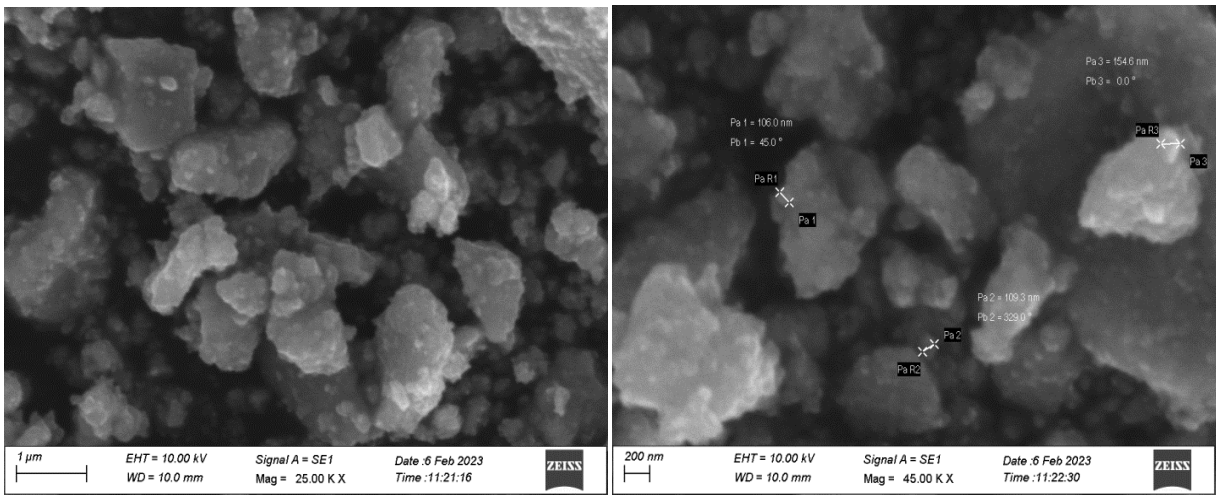

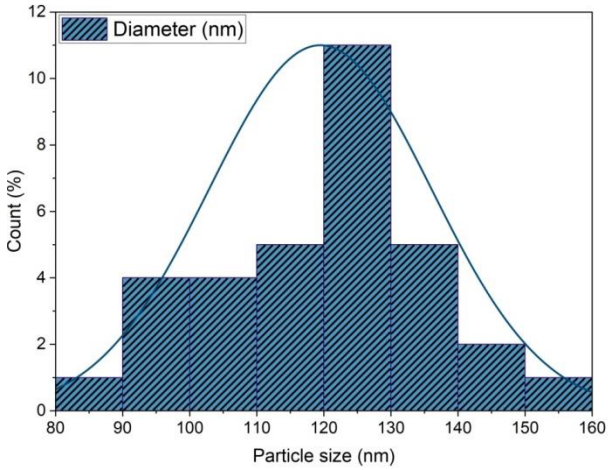

Figure 10.SEM imagesand histogram ofBi_2O_3NPs

3.2.5. EDA Xspectrum of Bi_2O_3NPs

The elemental and compositional properties of Bi_2O_3NPs were investigated by EDAX shown in figure 11. The spectrum showed the presence of Bi and O peaks which indicated the presence of pure Bi_2O_3NPs without any impurities and weight percentages of 72% and 28% for O and Bi respectively.

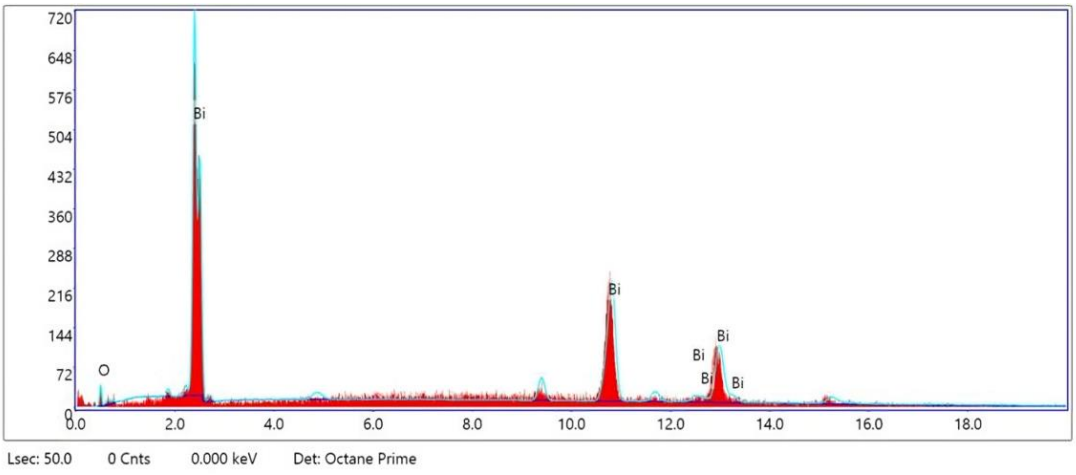

Figure 11. EDAX Spectra of Bi_2O_3NPs

3.2.6. BET Surface area analysis

BET surface area and pore volume of Bi_2O_3NPs was determined using standard N_2 adsorption-desorption method at STP showed in figure 12(A) & (B), which represented the N_2 adsorption-desorption isotherm plot and BET surface area plot. BET surface area of Bi_2O_3NPs was 23.6591 ± 0.4367 m²/g and its total pore volume was less than 1909.324 Å diameter at P/Po=0.989770885 and quantity adsorbed at STP=0.020829 cm³/g. N_2 adsorption and desorption isotherm was plotted which resembled the Type IV isotherm confirming the presence mesoporous structures [15]. Low pressure showed monolayer formation and inflection point occured at the completion of monolayer.

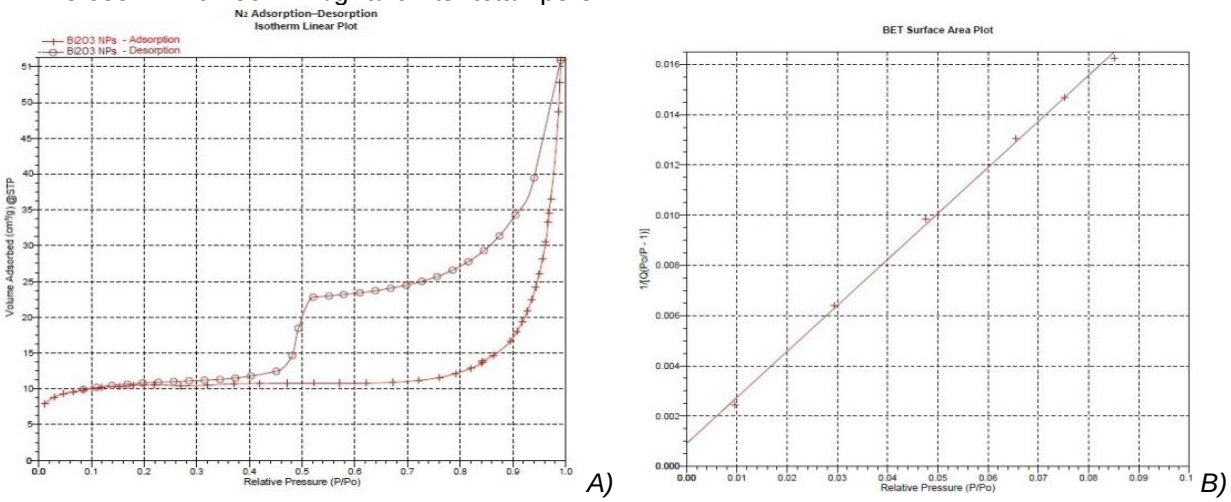

Figure 12. (A) N_2 adsorption–desorption isotherms linear plot. (B) BET surface area plot

3.3. Application-Adsorptionof RhB by Bi_2O_3NPs

Nowadays contagious diseases spread drastically ever before due to many environmental factors and one such prime element responsible is the spread through contaminated water. Currently arising worldwide issue is the poor accessibility to clean and safe drinking water. There is a requirement for sustainable water remediation technique and one such eminent method is adsorption. The dissolved contaminants (adsorbate) in solution when enter into close vicinity of the adsorbent, some of the contaminants gets adsorbed on the surface of the adsorbent through intermolecular force of attraction. One such adsorbent that provides an excellent adsorbing ability is a nanoparticle which has high surface area, more active site, many pores, low intra-species diffusion distance etc. [16]. Commonly known contaminants are textile dyes like RhB which are carcinogenic and creates neurological disorders in humans. In the present work Bi_2O_3NPs, a magnificent nano-adsorbent was utilized to adsorb RhB dye and the extent of adsorption was studied through the intensity of decolouration and the decrease of concentration identified through the decrease of absorbance in the UV-Vis spectra of treated RhB (λ_m=538 nm) [17] contaminated water.

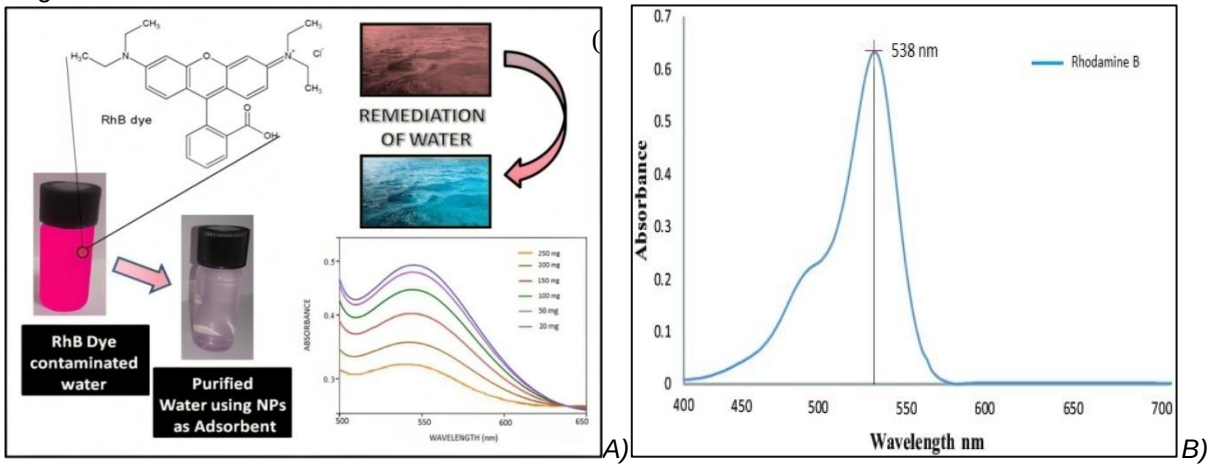

Figure 13. (A) Pictorial representation of RhB adsorption. (B) UV-Vis spectrum of RhB dye

Figure 13(A) illustrates a pictorial representation of RhB dye degradation and figure 13(B) shows the UV-Vis spectrum of RhB dye. The impact of various operational factors on the adsorption of nanoparticles by commercial organic dye was examined. These factors included effect of adsorbent dose, adsorbate dose, time, temperature, and pH of adsorption process.

3.3.1. Effect of adsorbent

The adsorption process was induced through Bi_2O_3NPs, varied from 20mg to 250mg and the RhB dye concentration was maintained as constant (20 ppm) at room temperature for 2 hrs. Table 2 shows the corresponding absorbance (a.u.) for various absorbent dosages in the adsorption process and figure 14 represents the plot between absorbance and adsorbent dosage. The results obtained showed greater adsorption efficiency of Bi_2O_3NPs towards the removal of RhB dye initially and later above 100mg of Bi_2O_3NPs the decrease of absorbance is moderate due to agglomeration of Bi_2O_3NPs after reaching optimum level [18].

Table 2. Absorbance value for various adsorbent dosage (in mg).

Adsorbent Dosage (mg)	Absorbance (a.u.)
20	0.471
50	0.463
100	0.406
150	0.394
200	0.389
250	0.372

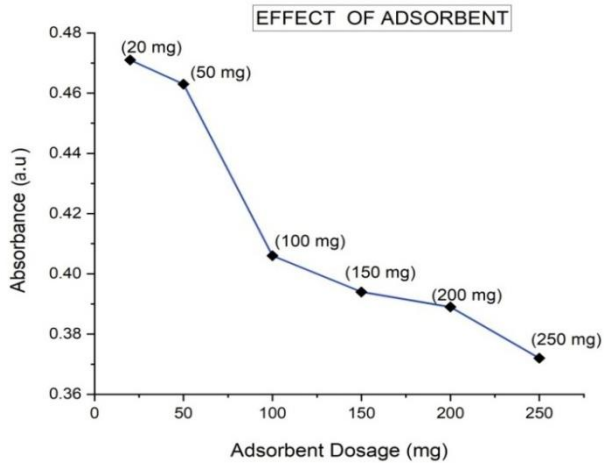

Figure 14. Plot between Absorbance and Adsorbent dosage (in mg).

3.3.2. Effect of adsorbate

RhB dye of different concentrations (10, 20, 30, 40, 50, 60 ppm) were utilized for the study of adsorption behaviors of Bi_2O_3 NPs and agitated at room temperature for 2hrs. The quantity of nanoparticles was maintained as 50 mg for all the adsorbate variation studies. Table 3 shows the corresponding absorbance (a.u.) for various absorbate dosages in the adsorption process and figure 15 represents the plot between absorbance and adsorbate dosage. On increasing the concentration of the dye the activity of adsorbent becomes negligible and inefficient. Initially the increases of concentration were gradual as the possible adsorption ability of Bi_2O_3 NPs played its role to adsorb. Later at high concentrations of dye, the adsorption process becomes incompetent and ultimately the absorbance also increases (gradually and then sharply).

Table 3. Absorbance value for various adsorbate dosages (in ppm)

Adsorbate Dosage (ppm)	Absorbance (a.u.)
10	0.401
20	0.425
30	0.441
40	0.521
50	0.565
60	0.635

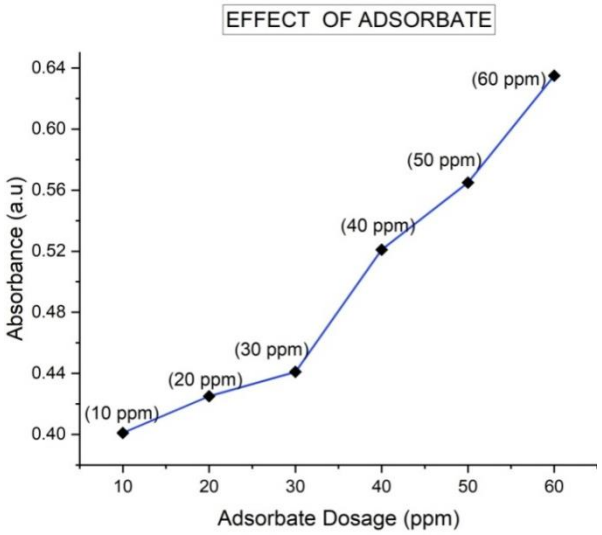

Figure 15. Plot between Absorbance and Adsorbate dosage (in ppm)

3.3.3. Effect of temperature

The temperature had a significant impact on adsorption, which was investigated by varying the temperature range from 30℃ to 80℃ and the concentration of Bi_2O_3 NPs and RhB maintained as constant. Table 4 shows the corresponding absorbance (a.u.) for temperature dependence in the adsorption process and figure 16 represents the plot between absorbance and temperature. It was observed that the adsorption of dye on NPs increased with an increase of temperature. A decrease in the concentration of dye could be

confirmed through the decrease of absorbance value [19]. The optimum temperature was found to be 70℃ and further increase of temperature showed only a gradual decrease.

Table 4. Absorbance value for effect of temperature (in ℃) variation in adsorption process

Temperature of Adsorption reaction (℃)	Absorbance (a.u.)
30	0.571
40	0.508
50	0.462
60	0.391
70	0.349
80	0.335

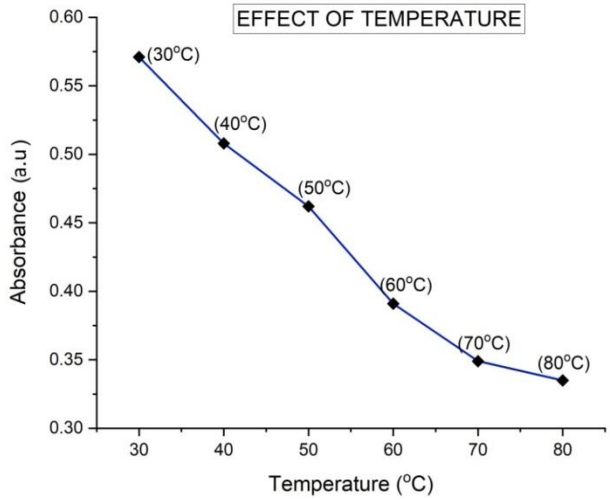

Figure 16. Plot between Absorbance and Temperature variation (in ℃)

3.3.4. Effect of time

Constant dosage of Bi_2O_3 NPs and RhB were agitated at room temperature with different time of reaction starting from 30mins to 150mins. Table 5 shows the corresponding absorbance (a.u.) for various time interval in the adsorption process and figure 17 represents the plot between absorbance and time dependence of adsorption. As the time of reaction increases, the quantity of dye adsorbed by NPs increases abruptly and then gradually which could be confirmed with the decrease of absorbance.

Table 5. Absorbance value for effect of time (in mins) variation in adsorption process

Time of Adsorption reaction (mins)	Absorbance (a.u.)
30	0.558
45	0.542
60	0.482
90	0.435
120	0.4
150	0.394

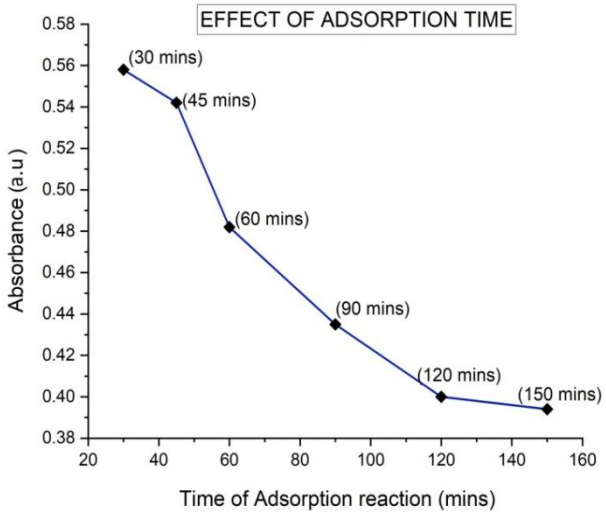

Figure 17. Plot between Absorbance and Time variation (in mins)

Constant dosage of Bi_2O_3 NPs and RhB were agitated at room temperature with different time of reaction starting from 30mins to 150mins. Table 5 shows the corresponding absorbance (a.u.) for various time interval in the adsorption process and figure 17 represents the plot between absorbance and time dependence of adsorption.As the time of reaction increases, the quantity of dye adsorbed by NPs increases abruptly and then gradually which could be confirmed with the decrease of absorbance.

3.3.5. Effect of pH

On varying the pH from 1 to 11, adsorbents demonstrated better adsorption capacity in basic medium than in acidic medium. Table 6 shows the corresponding absorbance (a.u.) for various pH in the adsorption process and figure 18 represents the plot between absorbance and pH dependence of adsorprtion. At basic medium, the accumulation of $-OH^{--}$ ions on the surface of the adsorbent attracts the cationic RhB dye and hence adsorption capacity increases. Since contaminants are wisely adsorbed, concentration of the solution decreases and thereby absorbance decreases [20].

Table 6. Absorbance value for pH change in adsorption process

pH of Adsorption reaction	Absorbance (a.u.)
1	0.428
3	0.403
5	0.384
7	0.376
9	0.359
11	0.347

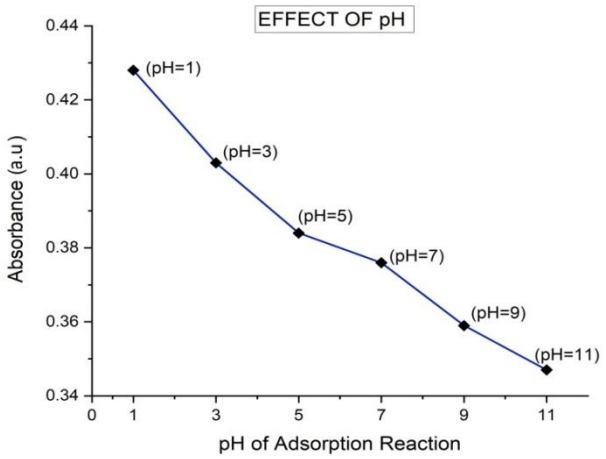

Figure 18. Plot between Absorbance and pH variation

4. CONCLUSION

This study has successfully extracted betacyanin from *Selenicereus undatus* peel extract and achieved in quantizing the maximum content of betacyanin. Further, *Selenicereus undatus* peel modified Bi_2O_3 NPs was synthesized and the formation of Bi_2O_3 NPs was confirmed through UV-Vis, FTIR, SEM, EDAX, XRD and BET surface area. A favorable adsorption method for removal of toxic dyes like RhB dye were investigated via green synthesized Bi_2O_3 NPs as nano-adsorbent and good adsorption behavior were shown. Hence, an incredible adsorption studies were established which could contribute to the sustainable development of the society.

Acknowledgement

The authors sincerely acknowledge the management and the Department of Chemistry, Holy Cross College (Autonomous), Trichy for their constant support and the facilities provided to carry out the research work.

5. REFERENCES

[1] T. Singh, V.K. Pandey, K.K. Dash, S. Zanwar, R.Singh(2023) Natural bio-colorant and pigments: Sources and applications in food processing, J. Agric. Food Res., 12, 100628. https://doi.org/10.1016/j.jafr.2023.100628

[2] P. Shanthy, J.A. Thangakani, S. Karthika, S.C. Joycee, S. Rajendran, J. Jeyasundari (2021) Corrosion inhibition by an aqueous extract of Ervatamia divaricata, Int. J. Corros. Scale Inhib., 10(1), 331–348. https://doi.org/10.17675/2305-6894-2021-10-1-19

[3] M.W. Alam, N. Allag, M. Utami, M. Waheed-Ur-Rehman, M. Al Saleh Al-Othoum, S. Sadaf (2024) Facile Green Synthesis of α-Bismuth Oxide Nanoparticles: Its Photocatalytic and Electrochemical Sensing of Glucose and Uric Acid in an Acidic Medium. Journal of Composites Science, 8(2),47-54. https://doi.org/10.3390/jcs8020047

[4] P. L. Meena, A.K. Surela, K. Poswal, J.K. Saini, L.K. Chhachhia (2024) Biogenic synthesis of Bi_2O_3 nanoparticles using Cassia fistula plant pod extract for the effective degradation of organic dyes in aqueous medium. Biomass Conversion and Biorefinery, 14(3), 3793-3809. https://doi.org/10.1007/s13399-022-02605-y

[5] A.O. Flayyih, W.K. Mahdi, Y.I.M.A. Zaid, F.H. Musa (2022) Biosynthesis, Characterization, and Applications of Bismuth Oxide Nanoparticles Using Aqueous Extract of Beta Vulgaris, Chem. Methodol., 6, 620-628. https://doi.org/10.22034/chemm.2022.342124.1522

[6] A. Pious, S. Muthukumar, D.K. Singaravelu, P. Nantheeswaran, M. Mariappan, A. Sivasubramanian, A. Veerappan (2024) Micelle assisted synthesis of bismuth oxide nanoparticles for improved chemocatalytic degradation of toxic Congo red into non-toxic products. New Journal of Chemistry, 48(1), 96-104. https://doi.org/10.1039/D3NJ04494G

[7] A.P Periyasamy (2024) Recent advances in the remediation of textile-dye-containing wastewater: prioritizing human health and sustainable wastewater treatment. Sustainability, 16(2), 495. https://doi.org/10.3390/su16020495

[8] K.P. Sambasevam, N. Yunos, H.N.M. Rashid, S.N.A. Baharin, N.F. Suhaimi, M. Raaov, S. Shahabuddin (2020) Evaluation of Natural Pigment Extracted from Dragon Fruit(Hylocereus Polyrhizus) Peels, Sci. Res. J., 17(2), 33-44. https://doi.org/10.24191/srj.v17i2.8989

[9] H.A. Alsalmah (2024) Structural, thermal, optical, morphological, electrical, and photocatalytic characteristics of silver-doped bismuth oxide synthesized by the green route. Ceramics International, 50(9), 14675-14685. https://doi.org/10.1016/j.ceramint.2024.01.380

[10] A.S. Ghorband, B. H. Joshi, H. G. Bhatt (2023) Studies on physicochemical and nutritional properties of dragon fruit (Hylocereus polyrhizus). Journal of Pharmacognosy and Phytochemistry, 12(6), 223-226. https://doi.org/10.22271/phyto.2023.v12.i6c.14785

[11] S. Lotfi, M.E. Ouardi, H.A. Ahsaine, A. Assani (2024) Recent progress on the synthesis, morphology and photocatalytic dye degradation of $BiVO_4$ photocatalysts: A review. Catalysis Reviews, 66(1), 214-258. https://doi.org/10.1080/01614940.2022.2057044

[12] C. Mallikarjunaswamy, S. Pramila, G.S. Shivaganga, H.N. Deepakumari, R. Prakruthi, G. Nagaraju, V.L. Ranganatha (2023) Facile synthesis of multifunctional bismuth oxychloride nanoparticles for photocatalysis and antimicrobial test. Materials Science and Engineering: B, 290, 116323. https://doi.org/10.1016/j.mseb.2023.116323

[13] N. Nurmalasari, Y. Yulizar, D.O.B. Apriandanu(2023)Bi_2O_3 nanoparticles: synthesis,

characterizations, and photocatalytic activity, IOP Conf. Ser.: Mater. Sci. Eng., 763, 012036. https://doi.org/10.1088/1757-899X/763/1/012036

[14] M. Alsaiari, M. Ahmad, M. Munir, M. Zafar, S. Sultana, S. Dawood, Z. Ahmad (2023) Efficient application of newly synthesized green Bi_2O_3 nanoparticles for sustainable biodiesel production via membrane reactor. Chemosphere, 310, 136838. https://doi.org/10.1016/j.chemosphere.2022.136838

[15] R. Ranjithkumar, C. Van Nguyen, L.S. Wong, J.G.T. Nandagopal, S. Djearamane, G. Palanisamy, J. Lee (2023) Chitosan functionalized bismuth oxychloride/zinc oxide nanocomposite for enhanced photocatalytic degradation of Congo red. International Journal of Biological Macromolecules, 225, 103-111. https://doi.org/10.1016/j.ijbiomac.2022.11.302

[16] Y. Zhu, L. Ma, L. Wang, X. Li, Z. Yang, M. Yuan, Y. Xiao (2024) Adsorption of Cationic Dyes in Wastewater with Magnetic κ-Carrageenan Nanoparticles. Process Safety and Environmental Protection,189, 177-187. https://doi.org/10.1016/j.psep.2024.06.039

[17] M. Lal, P. Sharma, L. Singh, C. Ram (2023) Photocatalytic degradation of hazardous Rhodamine B dye using sol-gel mediated ultrasonic hydrothermal synthesized of ZnO nanoparticles. Results in Engineering, 17, 100890. https://doi.org/10.1016/j.rineng.2023.100890

[18] A.Q. Malik, T.U.G. Mir, D. Kumar, I.A. Mir, A. Rashid, M. Ayoub, S. Shukla (2023) A review on the green synthesis of nanoparticles, their biological applications, and photocatalytic efficiency against environmental toxins. Environmental Science and Pollution Research, 30(27), 69796-69823. https://doi.org/10.1007/s11356-023-27437-9

[19] M.A Dheyab, N. Oladzadabbasabadi, A.A. Aziz, P.M. Khaniabadi, M.T. Al-ouqaili, M.S. Jameel, M. Ghasemlou (2024) Recent advances of plant-mediated metal nanoparticles: Synthesis, properties, and emerging applications for wastewater treatment. Journal of Environmental Chemical Engineering, 112345. https://doi.org/10.1016/j.jece.2024.112345

[20] A.S. Prabha, N. Vijaya, R. Dorothy, T. Sasilatha, T. Umasankareswari, R. Keerthana, N.R. Devi, S. Rajendran, G.Singh (2022) Use of Nanocomposites as Photocatalysts, Nanocomposites- Jenny Stanford Publishing, 13, 283-327. https://doi.org/10.1201/9781003314479

IZVOD

HIJERARHIJSKI OKVIR, IZRADA I KARAKTERIZACIJA NANO-Bi_2O_3 POSREDSTVOM EKSTRAKTA *SELENICEREUS UNDATUS* I NJEGOVA PRIMENA

Betacijanini (BC) su crvenkasto-ljubičasti pigment koji se široko nalazi u korama zmajevog voća sa belim mesom (Selenicereus undatus) i kore i pulpe crvenog zmajevog voća (Selenicereus costaricensis). BC pigmenti su dobri antioksidansi koji inhibiraju formiranje reaktivnih vrsta kiseonika (ROS) u biljkama i na taj način promovišu redukciju metalnih jona na nula valentnih metala. Takođe, deluje kao dobar stabilizator i agens za zatvaranje u sintezi nanočestica. Dakle, ovo istraživanje ima za cilj da ekstrahuje i kvantizuje sadržaj BC iz kore Selenicereus undatus, kako bi se proizvele nanočestice modifikovanih bizmut oksida (SU) bogate betacijaninom-Selenicereus undatus (Bi_2O_3 NP) i karakterisale korišćenjem UV-Vis, FTIR, XRD, SEM, EDAX i BET. Količina i stabilnost betacijanina se optimizuju korišćenjem različitih parametara kao što su vreme, temperatura, odnos rastvarača, pH, itd., preko UV-Vis spektrofotometra na 538 nm. Sintetizovani SU-Bi_2O_3 NP imaju za cilj ublažavanje zagađivača sintetičkih boja putem adsorpcije – efikasan put za remedijaciju vode. Nano-adsorbenti Bi_2O_3 NP su pokazali povećanje adsorpcije boje sa povećanjem vremena reakcije, temperature i doze Bi_2O_3 NP, što je omogućilo efikasno uklanjanje boja kao što su Rhodamine B (RhB) boje.

Ključne reči: *betacijanin, Selenicereus undatus, nanočestice bizmut oksida, karakterizacija, rodamin B boje.*

Naučni rad
Rad primljen: 05.06.2024
Rad prihvaćen: 01.07.2024.

Auxilia Ruby Sagaya Irudayaraj https://orcid.org/0000-0002-1636-1252
Felicita Florence John https://orcid.org/0000-0002-3255-5997
Divya Priya Chinnasamy -R. Kanmani https://orcid.org/ 0000-0002-9873-1324
Amala Infant Joice Joseph https://orcid.org/0000-0002-8661-2280